Indian Journal of Chemistry
Vol. 56A, August 2017, pp. 843-847

Synthesis of silver nanocatalyst in presence of poly(ethylene glycol) and its application for electrocatalytic reduction of hydrogen peroxide

Samira Ghasemi[a], Jahan Bakhsh Raoof[a,*], Fereshteh Chekin[b] & Reza Ojani[a]

[a]Electroanalytical Chemistry Research Laboratory, Department of Analytical Chemistry, Faculty of Chemistry, University of Mazandaran, Babolsar, Iran

Email: j.raoof@umz.ac.ir

[b]Department of Chemistry, Ayatollah Amoli Branch, Islamic Azad University, Amol, Iran

Received 29 January 2017; revised and accepted 31 July 2017

The synthesis of powdered Ag nanoparticles in presence of poly(ethylene glycol) as reducing agent and stabilizer in aqueous medium is reported. The structure and properties of the Ag nanoparticles have been characterised by X-ray diffraction, transmission electron microscopy and energy dispersive X-ray data. XRD study shows that the particles are crystalline in nature with face centered cubic geometry. Formation of stable silver nanoparticles gives mostly spherical particles with diameter in the range of 12–30 nm. The catalytic activity of the nanocrystalline AgNPs, for the reduction of hydrogen peroxide has been studied at the surface of glassy carbon electrode modified with Ag nanoparticles and poly(methyl methacrylate) (AgNPs-PMMA/GCE) prepared by casting of the AgNPs-PMMA solution on GCE. The sensor responds to H_2O_2 with high selectivity, good reproducibility and stability, over a linear range of 22–1700 μ*M* with a detection limit of 4.8 μ*M* using amperometry.

Keywords: Electrochemistry, Electrodes, Modified electrodes, Silver nanoparticles, Nanoparticles, Nanocatalysts, Poly(ethylene glycol), Hydrogen peroxide reduction

Metal nanomaterials have attracted wide interest for application in various fields. Among the metals, silver nanomaterials have exhibited the highest thermal and electrical conductivity and is widely used in electronics,[1] catalysis,[2] optics,[3] biological labeling,[4] surface-enhanced Raman scattering, etc.[5,6] Extensive works have been carried out to synthesize silver nanoparticles with controllable shape and size and desired electric and optical properties.[7-12] Various techniques such as chemical reduction,[13-18] electrochemical reduction,[19,20] photochemical reduction,[21,22] and heat evaporation[23,24] have been developed to synthesis metal nanoparticles. In most cases, in the chemical reduction of AgNPs, surface passive reagents to prevent nanoparticles from aggregation are needed. Unfortunately, many organic passive or reducing agents are toxic and pollute the environment if nanoparticles are produced in large scale.[25] Some methodologies like use of arginine, green tea, etc. as reducing agent and non-conventional heating techniques like microwaves.[26] have been reported to replace these toxic reducing agents.

Scalability of process and yield of naked (bare metal) nanoparticles, however, still remain a major concern. A suitable soluble polymer is usually added as a protective agent. In the absence of soluble polymer, the resultant particles are in the micrometer or sub-micrometer size range.[27-31] Poly(ethylene glycol) (PEG) is liquid or low-melting solid, depending on the molecular weight. PEGs are prepared by polymerization of ethylene oxide and are commercially available over a wide range of molecular weights from 300 g/mol to 10,000,000 g/mol. PEG with different molecular weights find use medical and clinical uses.[32]

Hydrogen peroxide is naturally produced in living organisms as a by-product of oxygen metabolism. Furthermore, hydrogen peroxide plays a role in oxidative stress as a reactive oxygen species (ROS). Hydrogen peroxide can be produced by enzymatic reaction. Hence, determination of hydrogen peroxide using AgNPs, can be performed in human body fluid.[33,34]

In this work, the synthesis of Ag nanoparticles was carried out in the presence of soluble polymer. The size and structure of the resultant nanoparticles were determined by TEM, XRD and EDAX. The catalytic property of synthesized Ag nanoparticles was examined by observing the reduction of hydrogen peroxide.

Experimental

Poly(ethylene glycol), poly(methyl methacrylate), hydrogen peroxide and silver nitrate were purchased from Aldrich. A stock solution of H_2O_2 was freshly diluted from 30% solution.

TEM images were recorded using LEO-Libra 120 transmission electron microscope. Hitachi S-3500N

scanning electron microscope with energy dispersive X-ray (EDAX) analysis was used for chemical characterization of the samples. The crystallization and purity of the synthesized samples were checked by X-ray diffraction. Electrochemical measurements were made with an Autolab Potentiostat/Galvanostat (Netherlands). The three-electrode system used in all voltammetric experiments consisted of an AgNPs-PMMA/GCE as working electrode, Ag|AgCl|KCl_{3M} as the reference electrode and a platinum wire as an auxiliary electrode (Metrohm).

The precursor solution to synthesize AgNPs was prepared by dissolving 3.0 g poly(ethylene glycol) in the 60 mL deionized water. The solution was stirred at 60 °C. Then, 20 mL silver nitrate solution (1.0 *M*) was added to the above solution with continuous stirring, after which the container was placed in a water bath at 80 °C. The stirring was continued overnight. The final product was calcined at 500 °C for 8 h to obtain silver nanoparticles.

For the fabrication of AgNPs-PMMA/GCE, appropriate amounts of Ag nanoparticles and PMMA were dispersed in 1 mL dimethylformamide (DMF) with the aid of ultrasonic agitation. The mass ratio of AgNPs:PMMA was 1:2. The mixture was sonicated for 20 min. Finally, a high dispersed colloidal solution was formed. Prior to use, the GC electrode (diameter 1.8 mm) was first polished with alumina (0.05 μm) slurry and ultrasonically cleaned with ethanol and doubly distilled water and then dried in room temperature. AgNPs-PMMA (5 μL) solution was coated on the GCE surface and dried in air.

Results and discussion

Figure 1 shows the XRD patterns of the AgNPs prepared in the presence of PEG. The XRD peaks in the wide angle range of 2θ (10° < 2θ< 90°) showed the peaks at 38.27°, 44.40°, 64.58° and 77.71° which may be attributed to 111, 200, 220 and 311, respectively of the face-central cubic (FCC) Ag structure (JCPDS: 87-0597).The (111) plane was chosen to calculate the crystalline size (either plane can be used for this purpose). By using Scherer's the average crystalline size for the AgNPs synthesized with PEG was determined to be approximately 15 nm.

Figure 2 shows the spherical morphology and size distribution of AgNPs prepared with PEG. The size histograms of the AgNPs are shown beside the relative TEM image. The histogram shows that the main particle size of the AgNPs prepared with PEG was about 18 nm. The EDAX is known to provide information on the chemical analysis of the fields that are being investigated or the composition at specific locations. The representative EDAX of the synthesized AgNPs shows that the prepared silver nanoparticles are free from other impurities (Fig. 3).

Cyclic voltammetry is one of the most common techniques, which used for determination of electroactivity behavior in electroanalytical chemistry. Figure 4 shows the cyclic voltammetric response obtained at the GCE and AgNPs-PMMA/GCE in

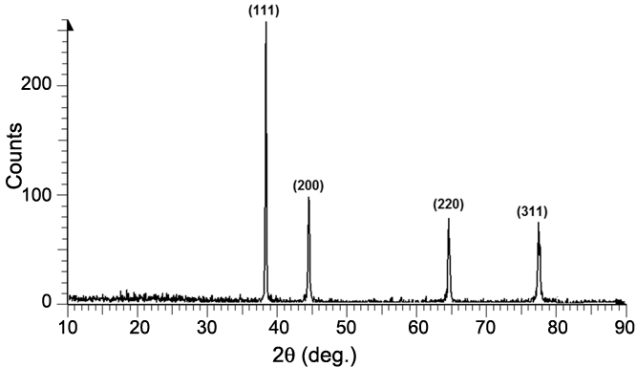

Fig. 1 – XRD pattern of synthesized AgNPs.

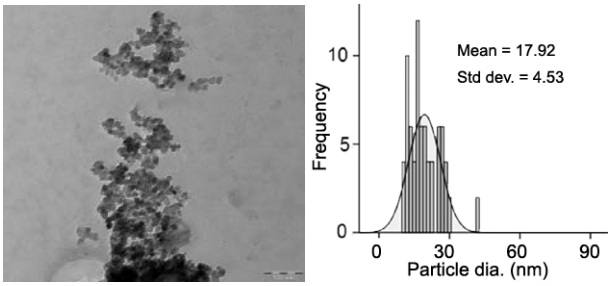

Fig. 2 – TEM image and histogram of the diameter distribution of synthesized AgNPs.

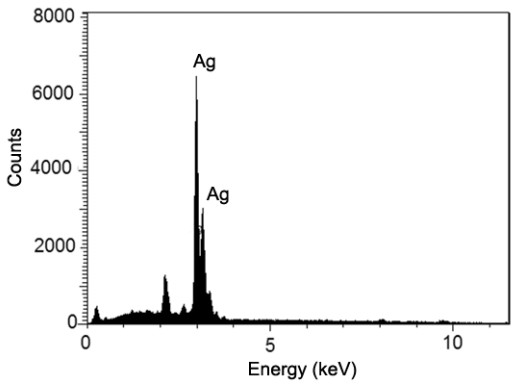

Fig. 3 – EDAX pattern of synthesized AgNPs.

0.1 *M* PBS (pH 7.00). At GCE (curves a), no obvious redox peak was observed but a couple of quasi-reversible and well-defined peaks with $E_{1/2}$ of 25 mV and ΔE of 190 mV were observed at 100 mV s^{-1} for AgNPs-PMMA/GCE (curve b) due to Ag nanoparticles.

The effect of the scan rates of potential on the cyclic voltammetric properties of AgNPs-PMMA/GCE was studied in 0.1 *M* PBS (pH 7.00) at various scan rates (Fig. 5). As can be seen, the values of anodic peak potential (E_{pa}) and cathodic peak potential (E_{pc}) shift slightly to the positive and negative directions, respectively, and the peak potential separation (ΔE_p) increases with increasing scan rate of potential. The anodic and cathodic peak currents are linearly proportional to scan rates of potential (Fig. 5, Inset), suggesting a surface-controlled process.

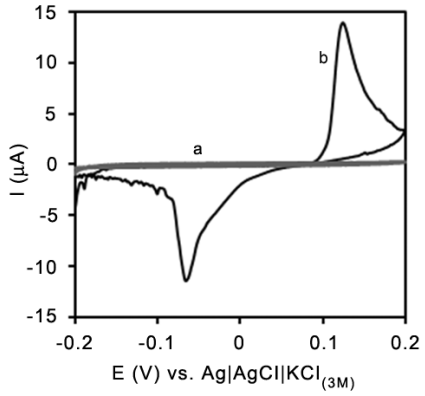

Fig. 4 – Cyclic voltammograms of (a) GCE and (b) AgNPs-PMMA/GCE in 0.1 *M* PBS solution (pH 7.00) and 0.1 *M* KCl as supporting electrolyte at scan rate of 50 mV s^{-1}.

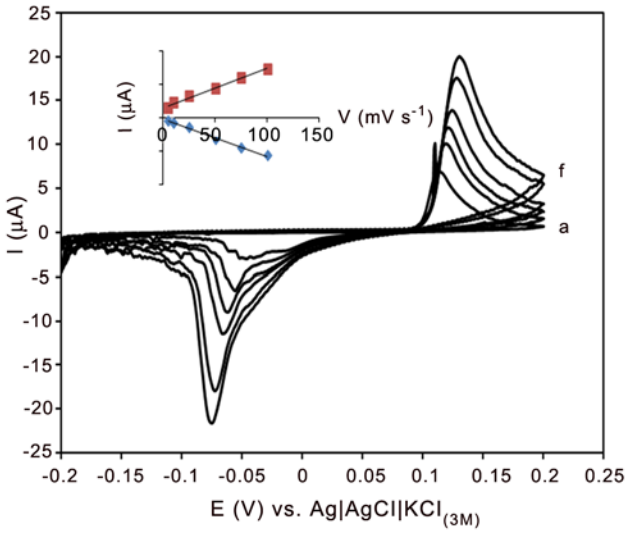

Fig. 5 – Cyclic voltammograms of AgNPs-PMMA/GCE in 0.1 *M* PBS solution (pH 7.00) and 0.1 *M* KCl as supporting electrolyte at various scan rates. [(a) 5, (b) 10, (c) 25, (d) 50, (e) 75, (f) 100 mV s^{-1}. Inset: Plot of variation of peak current versus scan rates of potential.

Figure 6 shows the cyclic voltammetric response obtained at the AgNPs-PMMA/GCE in the absence and presence of H_2O_2 in 0.1 *M* phosphate buffer solution (PBS, pH 7.00). As seen, the cyclic voltammogram (CV) of AgNPs-PMMA/GCE in 0.1 *M* PBS (pH 7.00) in the presence of 1.0 mM H_2O_2 (curve c) shows that the reduction peak increases greatly as compared with CV of GCE in the presence of H_2O_2

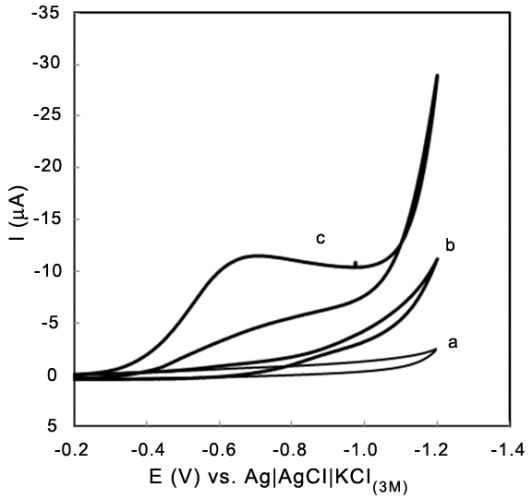

Fig. 6 – Cyclic voltammograms of (a) GCE in the absence of H_2O_2, (b) GCE in the presence of 1.0 m*M* H_2O_2 and (c)AgNPs-PMMA/GCE in the presence of 1.0 m*M* H_2O_2 in 0.1 *M* PBS solution (pH 7.00) and 0.1 *M* KCl as supporting electrolyte saturated with N_2 at scan rate of 50 mV s^{-1}.

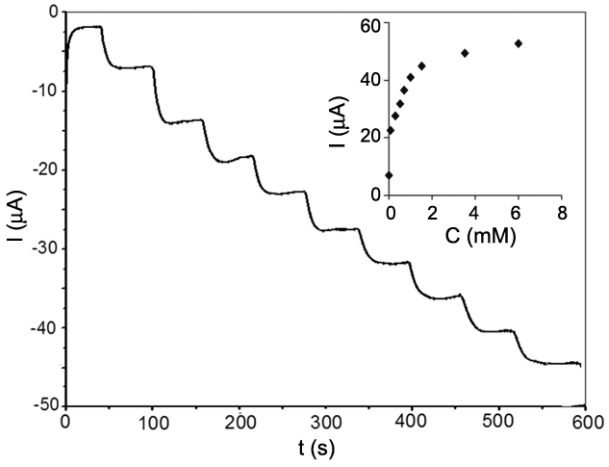

Fig. 7 – Current–time curve of AgNPs-PMMA/GCE with successive addition of H_2O_2 to a stirred N_2 saturation 0.1 *M* PBS (pH 7.00). [Inset is the calibration curve].

(curve b). The potential of reduction peak shifts positively. Obviously the AgNPs in AgNPs-PMMA composite deposited on GCE catalyzed the reduction of H_2O_2 and produced a remarkable catalytic current. The high catalytic current is mainly ascribed to the large surface-to-volume ratio of the small AgNPs which provided higher possibility to contact H_2O_2.

The amperometric response of the AgNPs-PMMA/GCE to successive additions of H_2O_2 stirred into 0.1 *M* PBS (pH 7.00) is shown in Fig. 7. The reduction current of AgNPs-PMMA/GCE rises sharply to reach a maximum steady-state value when H_2O_2 was added. The fast response was ascribed mainly to the fact that the AgNPs-PMMA increased the total surface area and enhanced the transfer of electrolyte and H_2O_2. The inset in Fig. 7 shows the corresponding calibration curve for electrochemical determination of H_2O_2. The response of AgNPs-PMMA/GCE was linear with H_2O_2 concentration from 22–1700 μ*M*, with detection limit of 4.8 μ*M* at a signal-to-noise ratio of 3 and sensitivity of 790.1 μA m*M* cm^{-2}, which is comparable to results reported for analytical determination of H_2O_2 at the surface of other different modified electrodes.[35–40]

In the present study, we report a novel synthesis protocol of preparing silver nanoparticles involving the reduction of silver nitrate in the presence of poly(ethylene glycol) as stabilizer and as reducing agent in aqueous medium. The prepared silver nanoparticles were characterized by TEM, XRD and EDAX, and their activity as an efficient nanocatalyst for the reduction and electrochemical determination of hydrogen peroxide was studied. The response of AgNPs-PMMA/GCE was linear for H_2O_2 in the range of 22–1700 μ*M*, with detection limit of 4.8 μ*M* at a signal-to-noise ratio of 3 and sensitivity of 790.1 μA m*M* cm^{-2} comparable with results reported in literature for analytical determination of H_2O_2 at the surface of other different modified electrodes. These silver nanoparticles may be used in effluent treatment process for reducing the microbial load, industrial and medical application.

References

1 Alshehri A H, Jakubowska M, Młożniak A, Horaczek M, Rudka D, Free C & Carey J D, *ACS Appl Mater Interfaces*, 4 (2012) 7007.

2 Sharma K, Singh G, Singh G, Kumar M & Bhalla V, *RSC Adv*, 5 (2015) 25781.

3 Mahmudin L, Suharyadi E, SetioUtomo A B & Abraha K, *J Modern Phy*, 6 (2015) 1071.

4 Ahmad N, Bhatnagar Sh, Ali S S & Dutta R, *Int J Nanomed*, 10 (2015) 7019.

5 Guo H, Xing B, Hamlet L C, Chica A & He L, *Sci Total Environ*, 554/555 (2016) 246.

6 Yang M, Zhang L, Chen B, Wang Zh, Chen Ch & Zeng H, *Nanotechnology*, 28 (2017) 055301.

7 Sherry L J, Chang SH, Schatz G C, Van Duyne R P, Wiley B J & Xia Y, *Nano Lett*, 5 (2005) 2034.

8 Wiley B J, Im S H, Li Z Y, McLellan J, Siekkinen A & Xia Y, *J Phys Chem, B*110 (2006) 15666.

9 Lu L, Kobayashi A, Tawa K & Ozaki Y, *Chem Mater*, 18 (2006) 4894.

10 Maillard M, Huang P & Brus L, *Nano Lett*, 3 (2003) 1611.

11 Hu J, Chen Q, Xie Z, Han G, Wang R, Ren B, Zhang Y, Yang Z & Tian Z, *Adv Funct Mater*, 14 (2004) 183.

12 Ni C, Hassan P A & Kaler E W, *Langmuir*, 21 (2005) 3334.

13 Sre P R R, Reka M, Poovazhagi R, Kumar M A & Murugesan K, *Spectrochim Acta: A*, 135 (2015) 1137.

14 Mahdi S, Taghdiri M, Makari V & Rahimi-Nasrabadi M, *Spectrochim Acta: A*, 136 (2015) 1249.

15 Bindhu M R & Umadevi M, *Spectrochim Acta: A*, 135 (2015) 373.

16 Ahmed Sh, Mudasir Ahmad S, Swami B L & Ikram S, *J Radiat Res Appl Sci*, 9 (2016) 1.

17 Bhui D K, Bar H, Sarkar P, Sahoo G P, De S P & Misra A, *J Mol Liq*, 145 (2009) 33.

18 Chekin F & Ghasemi S, *Bull Mater Sci*, 37 (2014) 1433.

20 Virginia Roldán M, Pellegri N & de Sanctis O, *J Nanoparticles*, 2013 (2013) 7.

20 Treshchalov A, Erikson H, Puust L, Tsarenko S, Saar R, Vanetsev A, Tammeveski K & Sildos I, *J Coll Inter Sci*, 491 (2017) 358.

21 Shvalagin V V, Grodzyuk G Y, ShvetsA V , Granchak V M, LavorikS R & Skorik N A, *Theoret Exp Chem*, 51 (2015) 177.

22 Elsupikhe R F, Ahmad M B, & Shameli K, *IEEE Trans Nanotechnol*, 15 (2016) 209.

23 Sopousek J, bursik J, Zalesak J & Pesina Z, *J Min Metal Sect B-Metal*, 48 (2012) 63.

24 Mirzaee M & Dolati A, *J Nanopart Res*, 16 (2014) 2582.

25 Bar H, Bhui D K, Sahoo G P, Sarkar P & Pyne S, *Physicochem Eng Aspects*, 384 (2009) 212.

26 Moulton M C, Braydich-Stolle L K, Nadagouda M N, Kunzelman S, Hussain S M & Varma RS, *Nanoscale*, 2 (2012) 763.

27 Hegde M S, Larcher D, Dupont L, Beaudoin B, Tekaia-Elhsissen K & Tarascon J M, *Solid State Ionics*, 93 (1997) 33.

28 Silvert P Y, Herrera-Urbina R, Duvauchelle N, Vijayakrishnan V & Elhsissen K T, *J Mater Chem*, 6 (1996) 573.

29 Silvert P Y & Elhsissen K T, *Solid State Ionics*, 82 (1995) 53.

30 Fievet F, Lagier J P, Blin B, Beaudoin B & Figlarz M, *Solid State Ionics*, 32/33 (1989) 198.

31 Degen A & Maˇcek J, *Nanostruct Mater*, 12 (1999) 225.

32 Nalam P C, Clasohm J N, Mashaghi A & Spencer N D, *Tribol Lett*, 37 (2009)5 41.

33 Hsu ChCh, Lo Y R, Lin Y Ch, Shi Y C & Li P L, *Sensors*, 15 (2015) 25716.

34 Shariati-Rad M, Irandoust M & Salarmand N, *Aust J Anal Pharm Chem*, 2 (2015) 2381.

35 Song Y, Cui K, Wang L & Chen S, *Nanotechnol*, 20 (2009) 105501.
36 Chen H, Zhang Z, Cai D, Zhang S, Zhang B, Tang J & Wu Z, *Talanta*, 86 (2011) 266.
37 Lu W, Luo Y, Chang G, Liao F & Sun X, *Thin Solid Films*, 520 (2011) 554.
38 Lin C Y, Lai Y H, Balamurugan A, Vittal R, Lin C W & Ho K C, *Talanta*, 82 (2010) 340.
39 Liu S, Wang L, Tian J, Luo Y, Zhang X & Sun X, *J Colloid Interf Sci*, 363 (2011) 615.
40 Wu S, Zhao H T, Ju H X, Shi C G & Zhao J W, *Electrochem Commun*, 8 (2006) 1197.